

Crystallization of Antimicrobial Pores in Membranes: Magainin and Protegrin

Lin Yang,* Thomas M. Weiss,* Robert I. Lehrer,[†] and Huey W. Huang*

*Physics Department, Rice University, Houston, Texas 77251-1892; and [†]Department of Medicine, UCLA School of Medicine, Los Angeles, California 90095 USA

ABSTRACT Membrane pores spontaneously formed by antimicrobial peptides in membranes were crystallized for the first time by manipulating the sample hydration and temperature. Neutron diffraction shows that magainins and protegrins form stable pores in fully hydrated fluid membranes. At lower hydration levels or low temperature, the membrane multilayers crystallize. In one crystalline phase, the pores in each bilayer arrange in a regular hexagonal array and the bilayers are stacked into a hexagonal ABC lattice, corresponding to the cubic close-packed structure of spheres. In another crystalline phase, the bilayers are modulated into the rippled multilamellae, corresponding to a 2D monoclinic lattice. The phase diagrams are described. Crystallization of the membrane pores provides possibilities for diffraction studies that might provide useful information on the pore structures.

INTRODUCTION

One remaining major challenge in structural biology is solving the structures of proteins and protein assemblies in membranes. In recent years, we have made progress in detecting and analyzing the structures of peptide assemblies in fluid membranes by neutron diffraction (He et al., 1995, 1996a; Ludtke et al., 1996; Yang, L. et al., 1998, 1999). These experiments were performed with membranes in the form of oriented multilayers. Originally the samples were investigated in full hydration so that the physical properties of the lipid bilayers were close to the physiological conditions. However, it was soon realized that the sample hydration is a useful experimental parameter. New phenomena of peptide-lipid interactions were discovered when the sample hydration was varied. In general, in full hydration, the peptide organization in each lipid bilayer is uncorrelated to the neighboring bilayers. However as the hydration level decreases, the peptide organizations become correlated between bilayers, even though the membranes are still fluid. In many cases, further dehydration strengthens the correlation such that the peptide organization in the multilayers crystallizes (Yang, L. et al., 1999). This was a rather unexpected result. The crystals are not those of the peptides alone. They are crystals of peptide-lipid assemblies within lipid bilayers. Such crystals have not been reported before. These new phases provide the possibilities for diffraction studies of supramolecular peptide assemblies in lipid bilayers. In this paper, we will describe an efficient way of controlling the sample hydration to investigate the crystalline phases using neutron or x-ray diffraction. A facility capable of rapid, continuous change of the sample hydration is essential for

this experiment. We will describe the crystal phases we have observed and the phase diagrams of the crystalline phases for two antimicrobial peptides in phospholipid bilayers. The crystalline samples are thin and are supported on a substrate that presents a challenge to diffraction studies. This problem will also be discussed.

Antimicrobial peptides are inducible innate host defense molecules found first in insects (Steiner et al., 1981) and subsequently in all multicellular organisms that were investigated, including humans and plants (Ganz and Lehrer, 1998; Hoffmann et al., 1999). These peptides are typically 20 to 40 amino acids long, with a folded size comparable to the membrane thickness. All evidence indicates that antimicrobial peptides act by permeabilizing the cell membranes of microorganisms (see reviews in Boman et al., 1994), although, in addition, receptor-mediated signaling activities of some peptides have been reported (Yang, D. et al., 1999; Hoffmann et al., 1999). In particular, synthetic all-D amino acid enantiomers of the peptides, including magainin (Wade et al., 1990; Bessalle et al., 1990) and protegrin (Yasin et al., 1996; Cho et al., 1998), have exhibited the same antimicrobial spectrum as their all-L native peptide counterparts. This indicates that the action of antimicrobial peptides does not involve stereo-specific protein receptors; rather, the action is the result of direct interaction with the lipid matrix of the plasma membrane.

All the peptides we have investigated, including alamethicin (Huang and Wu, 1991), magainins (Ludtke et al., 1994), protegrins (Heller et al., 1998), and melittin (Harroun, 1999), exhibit two distinct oriented circular dichroism (OCD) spectra (Wu et al., 1990) when they are bound to membranes, one at low peptide-to-lipid ratios (P/L) and another at high P/L. This indicates that each peptide has two distinctly different physical states of binding to a membrane. The transition from the low to the high P/L state takes place over a narrow range of P/L as if there is a threshold concentration, called P/L* (Huang and Wu, 1991; Heller et al., 1998). P/L* for each peptide varies greatly with the lipid

Received for publication 29 March 2000 and in final form 20 June 2000.

L. Y. and T. M. W. contributed equally to this work.

Address reprint requests to Dr. Huey W. Huang, Physics Department, Rice University, Houston, TX 77251-1892. Tel: 713-348-4899; Fax: 713-348-4150; E-mail: hw Huang@rice.edu.

© 2000 by the Biophysical Society

0006-3495/00/10/2002/08 \$2.00

composition of the membrane (Huang and Wu, 1991; Ludtke et al., 1994; Heller et al., 1998). At concentrations below P/L^* , the peptides are embedded in the lipid head group region, called the surface state, as suggested by the peptide orientation and the membrane thinning effect (Wu et al., 1995; Ludtke et al., 1996; Heller et al., 2000). At concentrations above P/L^* , neutron in-plane scattering showed that the peptides form pores in the membranes, whereas no pores were detected below P/L^* (He et al., 1995, 1996a; Ludtke et al., 1996). The majority of the peptides at concentrations above P/L^* are in the pore state. Pore formation in such high densities is stable, contrary to what is observed in single-channel experiments where extremely low peptide concentrations are used and the pore formations are fluctuation phenomena (Christensen et al., 1988; Duchohier et al., 1989; Sokolov et al., 1999). The pores observed by neutron have diameters of ~ 20 Å or larger. Massive pore formations are apparently lethal if they occur in cell membranes. We concluded that pore formation is the mode of action of antimicrobial peptides, and the control of P/L^* by the cell membrane's lipid composition could be the gating mechanism (He et al., 1996b; Ludtke et al., 1996; Heller et al., 1998, 2000; Huang, 2000).

The direct observation of pores in fluid membranes is important, because it is related to the physiological condition of membranes. This was achieved by exploiting the sensitivity of neutron to D_2O , which had replaced the water in the membrane pores. However, diffraction from the fluid state allowed only an estimate of the pore size (He et al., 1996a). The diffraction signals from fluid membranes were limited to a low range of q (the momentum transfer of scattering), which made detailed structural analyses of the pores difficult. To understand the energetics of the pore formation and the gating mechanisms of the antimicrobials' activity, it is imperative to know the structures of the pores. Thus, we believe that the discovery of the crystalline phase is an important new development for the field of antimicrobial peptides.

Two peptides isolated from animals were selected for investigation by this novel approach. Magainin 2 (NH_2 -Gly-Ile-Gly-Lys-Phe⁵-Leu-His-Ser-Ala-Lys¹⁰-Lys-Phe-Gly-Lys-Ala¹⁵-Phe-Val-Gly-Glu-Ile²⁰-Met-Asn-Ser-CONH₂) is a 23-residue peptide secreted by the skin of the African clawed frog *Xenopus laevis* (Zasloff, 1987). In vitro, it exhibits broad-spectrum antibacterial, antifungal, and tumoricidal activities (Zasloff, 1987; Cruciani et al., 1991). Protegrin-1 (PG-1) (NH_2 -Arg-Gly-Gly-Arg-Leu⁵-Cys-Tyr-Cys-Arg-Arg¹⁰-Arg-Phe-Cys-Val-Cys¹⁵-Val-Gly-Arg-CONH₂) is an 18-amino acid peptide isolated from the leukocytes of pigs (Kokryakov et al., 1993). In vitro, PG-1 can kill many bacteria, including *Escherichia coli*, *Listeria monocytogenes*, and *Neisseria gonorrhoeae* (Kokryakov et al., 1993; Harwig et al., 1996; Qu et al., 1996, 1997). It is also active against the fungus *Candida albicans* (Kokryakov et al., 1993; Cho et al., 1998) and can protect cells from infection by human immunodeficiency

virus (Tamamura et al., 1995). One synthetic analogue of PG-1, IB367 (NH_2 -Arg-Gly-Gly-Leu-Cys⁵-Tyr-Cys-Arg-Gly-Arg¹⁰-Phe-Cys-Val-Cys-Val¹⁵-Gly-Arg-CONH₂), is also included for comparative studies. It is apparent that all these peptides have potential for pharmaceutical applications.

Magainin and protegrin represent two major classes of antimicrobial peptide structures. Magainin 2 adopts a primarily α -helical secondary structure upon binding to membranes (Matsuzaki et al., 1989; Williams et al., 1990; Ludtke et al., 1994). On the other hand, the NMR solution structure of PG-1 is a one-turn β hairpin in which the four cysteines form two disulfide bonds that stabilize the β sheet structure like two rungs of a ladder (Aumelas et al., 1996; Fahrner et al., 1996). It is reasonable to assume that this solution structure remains essentially unchanged when PG-1 binds to membranes, although this is yet to be shown by experiment. We also assume that the analogue IB-367 has the same conformation as PG-1, based on their analogy in amino acid sequence and the similarity between their CD spectra (Heller et al., 1998, and unpublished data).

EXPERIMENTAL

Magainin 2 amide was a gift from Drs. Michael Zasloff and W. Lee Maloy of Magainin Pharmaceuticals, Inc. (Plymouth Meeting, PA). Protegrin-1 and its synthetic analogue, IB367, were a gift from Dr. John Fiddes of IntraBiotics Pharmaceuticals, Inc. (Mountain View, CA). 1,2-Dimyristoyl-sn-glycero-3-phosphatidylcholine (DMPC) and 1,2-dimyristoyl-sn-glycero-3-phosphatidylglycerol (DMPG) were purchased from Avanti (Alabaster, AL). Quartz plates of 21 mm diameter and 0.25 mm thickness were purchased from Chemglass (Vineland, NJ). Silicon wafers with (100) surface were purchased from Semiconductor Processing (Boston, MA). All other chemicals were reagent grade. All materials were used as delivered.

Neutron diffraction

Sample preparation

The key to this experiment is a novel sample configuration. Its design was based on the following considerations. Neutron experiment typically requires a large amount of sample. The amount is determined by the signal-to-noise ratio, which increases proportionally to the square root of the scan time. For practical purposes, it is desirable to limit the collection time for a complete diffraction pattern of a sample to within 1 hour. Using the SANS beamline NG3 of the National Institute of Standards and Technology (NIST; Gaithersburg, MD) as a reference, this means that each sample requires at least 10 mg of lipid at the peptide-to-lipid molar ratios $P/L = 1/40$ to $1/10$. This amount of peptide-lipid mixture will be spread over several quartz plates, each with a sample area ~ 300 mm², so the total sample thickness

is about 30 μm . In our previous experiments, we divided ~ 50 mg sample into 6 or 7 separate layers and sandwiched each layer between two quartz plates (He et al., 1996a). Samples in this form can be aligned into uniformly oriented multilamellae, parallel to the substrate surfaces, by a number of techniques (Powers and Pershan, 1977; Huang and Olah, 1987). Most of our previous neutron experiments were performed with such sandwiched samples (He et al., 1995, 1996a; Ludtke et al., 1996; Yang, L. et al., 1998, 1999). However, it would take hours or days to change the hydration level of a sandwiched sample, too long for the conduct of a neutron experiment if hydration change is desired. In recent years, we have developed procedures for preparing thin oriented samples on a single substrate (Ludtke et al., 1995). Exposing such an open sample to a controlled water vapor pressure, one can change its hydration level within minutes. Open samples have been used in our lab for OCD experiments (Heller et al., 1997, 1998) and x-ray experiments (Ludtke et al., 1995; Chen et al., 1997; Harroun et al., 1999; Heller et al., 2000). However, the samples for OCD and x-ray experiments are typically 1 μm thick. It was not clear before this experiment if thick (~ 5 μm) samples can be aligned by the one-substrate preparation. Here we report the use of one-substrate sample for neutron experiment for the first time. All samples were prepared in conditions that have been examined by OCD previously, and the measurements indicated that the peptides were in the inserted state (Ludtke et al., 1994; Heller et al., 1998).

Quartz plates were cleaned abrasively and then soaked in a heated bath of sulfuric acid and chromic acid mixture for 15 to 20 min, followed by repeated washing with distilled H_2O and ethanol. Two micrograms of the lipid-peptide mixture was deposited on one plate from a stock solution of organic solvent. The concentration of the stock solution was ~ 10 mg/ml (lipid/solvent). As described in Ludtke et al. (1995), the final distribution of the material on the quartz surface depends strongly on the solvent used. The solution should have an appropriate surface tension with an appropriate evaporation rate to produce a uniform coating. We found that combinations of trifluoroethanol and chloroform worked for DMPC/magainin and DMPC/protogrin mixtures. For each sample composition, the ratio between the two solvents must be adjusted, by trial and error, to obtain the best results. The deposit dried to a visually smooth and uniform coating on the surface of the quartz plate. The sample was then placed in a freeze-dryer to remove any remaining trace of solvent. Six quartz plates, each with a uniform coating of the peptide-lipid mixture, were stacked in a pile. An aluminum spacer around the edge of the plate kept the plates from touching each other, and it also provided good thermal contact between the sample and the temperature-controlled sample mount. The space between plates allowed the deposited peptide-lipid multilayers to be in direct contact with water vapor. The stacked pile was

positioned in the neutron beam so that the quartz plates were first oriented perpendicular to the beam, then rotated by an angle ω with respect to an axis parallel to the plates and through the center of sample (see the sample geometry in Fig. 1 of Yang et al., 1998). The neutron beam was adjusted to a diameter of 8 mm. Care was taken to keep the aluminum spacers out of the neutron beam to avoid small-angle scattering signals from aluminum.

Temperature/humidity chamber

During the neutron experiment, the sample was housed in a temperature/humidity chamber equipped with quartz windows to allow the passage of incident and scattered neutron beam. The chamber consists of a sample mount at the center, which allows the sample to rotate as described, a pair of temperature and humidity probes, and a water bath. The construction is covered by two boxes, one inside the other so the inside box is thermally insulated from room temperature. The temperature and humidity controls are feedback circuits that respond to the outputs of the temperature and humidity probes. The feedback circuits provide heating or cooling using thermoelectric modules (Melcor Electronics Corp., Trenton, NJ). The temperature controller maintains the temperature of the sample mount. The device for the humidity control heats or cools a small water bath (D_2O was used in neutron experiment) that is positioned away from the sample mount. The temperature probe is an AD590 two-terminal IC temperature transducer, calibrated at 0°C with a mixture of ice and water and at 35°C with a calibrated Fisher digital thermometer. The probe was in direct contact with the sample mount. The relative humidity probe is model EMD-2000 (General Eastern Instruments, Woburn, MA). The relative humidity (RH) was calculated based on the impedance-RH table provided with the probe. In the chamber, the probe was positioned close to the sample. The humidity control heats or cools the water bath if the probe is lower or higher, respectively, than the set value for humidity. This device changes the temperature and humidity to a set value within minutes. The neutron diffraction pattern of the sample changed with temperature and humidity instantaneously. It remained unchanged after the temperature and humidity reached the set values. The temperature of the sample mount can be controlled to within $\pm 0.1^\circ\text{C}$. The RH in the vicinity of sample can be controlled to within $\pm 0.5\%$ RH in most cases.

X-ray diffraction

For x-ray diffraction experiment, 1 mg of peptide-lipid mixture was deposited on a silicon wafer over an area 10×30 mm^2 . A point source of Cu K_α radiation (operating at 35 mA/40 kV) was used. A thin Ni filter was placed at the tube exit to remove most of the Cu K_β radiation. The beam was then focused by a pair of spherically bent x-ray mirrors

(Charles Supper Co., MA). The mirrors were Ni-coated to further reduce the amount of K_{β} radiation. A temperature/humidity chamber similar to the neutron device described above was positioned on a goniometer head. X-ray diffraction was recorded on a Siemens X1000 multiwire proportional chamber (512×512 pixel; Bruker AXS Inc., Madison, WI) at the sample-to-detector distance of 21.54 cm. The distance was measured using sucrose powder as a calibration standard. A cone-shaped helium path covered the space between the chamber and the detector. X-ray samples were oriented at a grazing angle. Data collection time depends on the amount and quality of the sample. It is usually 20 min.

Two main differences between x-ray and neutron diffraction are: (1) Neutron, with the use of D_2O , is sensitive to both the fluid and crystalline states of membranes. X-ray is sensitive only to the crystalline state of membranes. (2) X-ray diffraction was measured by the reflection mode. It is difficult to find a suitable substrate that is transparent to x-ray. In contrast, quartz substrate is essentially transparent to neutron, hence both the transmitted and reflected neutron were recorded.

The techniques of measuring diffraction patterns from oriented multilayers have been described in two recent publications (Yang, L. et al., 1998, 1999). In particular, the full procedure for data reduction is given in Yang et al. (1998).

RESULTS AND DISCUSSION

In a previous paper (Yang, L. et al., 1999) we reported how the diffraction pattern of a magainin sample changed with hydration. When the membranes were fluid and fully hydrated, the diffraction pattern usually had a peak on the q_r axis ($q_z = 0$). (q_z and q_r are the projections of the momentum transfer of neutron or x-ray scattering perpendicular and parallel to the plane of bilayers, respectively.) This was interpreted as a result of in-plane scattering of D_2O -filled pores that were moving randomly in each bilayer. The in-plane positions of the pores in fluid membranes were uncorrelated between adjacent bilayers. When the hydration level was slightly less than full, the diffraction peak shifted off the $q_z = 0$ line (Fig. 1 B_1 , left panel). This means that the in-plane positions of the pores became correlated between adjacent bilayers, even though the diffraction was otherwise fluid-like, indicating that the bilayers were still in the fluid state. The cause of this correlation was speculated to be the hydration force (Yang, L. et al., 1999). Upon further dehydration or cooling, the correlation became long-range, and the diffraction pattern turned into sharp peaks (Fig. 1 B_1 , middle and right panels). Note that the diffraction peaks shown in the middle panel of Fig. 1 B_1 appeared to emerge directly from the fluid-like broad bands shown in the left panel as the sample was dehydrated or cooled, indicating that the scattering objects are the same for these two pat-

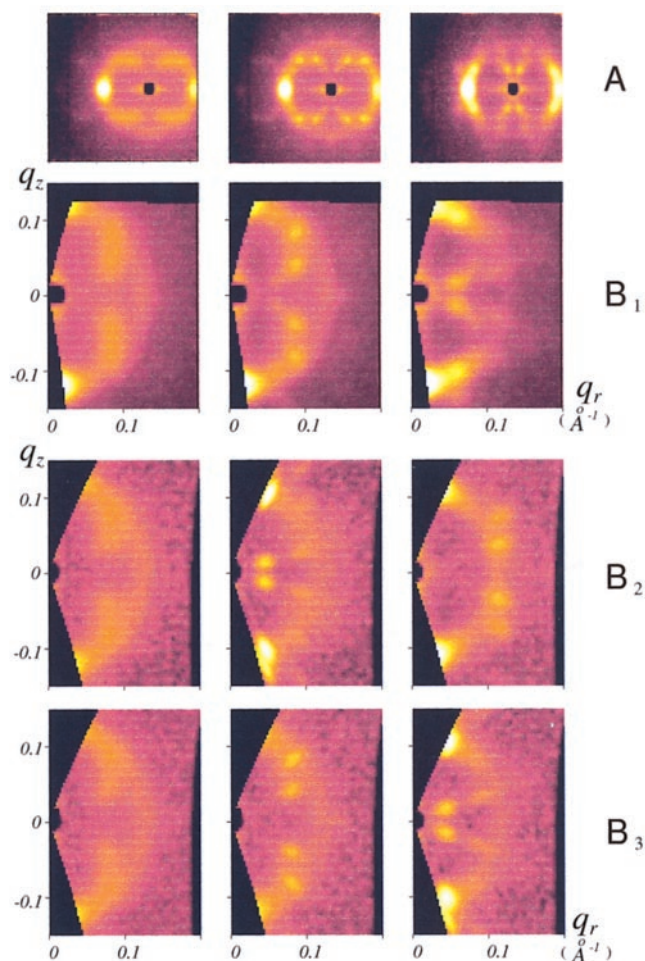


FIGURE 1 Neutron diffraction patterns of magainin, protegrin-1, and IB367 in DMPC. (A) Raw data on the area detector produced by magainin in DMPC at the peptide-to-lipid molar ratio (P/L) 1/30, measured at the sample tilt angle $\omega = 75^\circ$ (see the diffraction geometry in Yang et al., 1998). The patterns were not centered because the detector was displaced transversely to the beam direction to extend the q range. (B₁) The raw data shown in A were translated to the q_z - q_r plane. As temperature and/or the hydration level decreased from left to right, the sample showed three distinct patterns: membrane pores in fluid bilayers (*left panel*), crystalline of hexagonal ABC stacking (*middle panel*), and crystalline of 2D monoclinic (*right panel*). (B₂) Three patterns of protegrin-1 in DMPC (P/L = 1/30). Note that the sequence of appearance for the hexagonal ABC stacking and the 2D monoclinic is reversed, compared with magainin. (B₃) Three patterns of protegrin analogue IB367 in DMPC (P/L = 1/30). Note that the sequence is the same as magainin, but different from protegrin-1.

terns. When the hydration and/or temperature were decreased further, the crystal pattern in the middle panel turned into another crystal pattern, shown in the right panel. Within the ranges of temperature and hydration we explored in this experiment (see the phase diagram below), magainin in DMPC exhibited three phases: fluid phase and two crystalline phases of different symmetry.

The crystalline phases are not unique to magainin. Protegrin and its analogue, IB-367, also produced similar crys-

talline patterns (Fig. 1, B_2 and B_3). In contrast, no such patterns by alamethicin samples have been observed so far. Perhaps this indicates that protegrins and magainin form the same type of membrane pores (the toroidal pores; see Ludtke et al., 1996), differing from that of alamethicin (the barrel-stave pores; see He et al., 1996a). However, as will be discussed below, the phase diagram of protegrin is very different from that of magainin.

Hexagonal ABC stacking

The crystal pattern shown in the middle panel of Fig. 1 B_1 was examined over a wider q range by x-ray. The diffraction pattern on the area detector is shown in Fig. 2 A, left. The pattern was translated to the q_r - q_z plane by the method described in Yang et al. (1998) in Fig. 2 A, right. To understand this diffraction pattern, imagine equivalent magainin pores arranged on a regular hexagonal lattice in each bilayer. Fig. 3 shows a schematic for such a lattice on a realistic scale. The size of the magainin pores was determined by the analysis of in-plane scattering (Ludtke et al., 1996). The pore structure was a conjecture, based on indirect evidence, in which the lipids bend continuously from the top to the bottom monolayer through the pore (the toroidal model) with approximately

seven magainin monomers (the cylinders in the figure) packed in the lipid head group region around the hole (Ludtke et al., 1996). The orientation of the helical peptide was determined by OCD (Ludtke et al., 1994). Note that the pores in Fig. 3 are shown rotationally disordered, which may be the case in real samples. The lattice constant (denoted as a in Eq. 1 below) is determined by the diffraction data shown in Fig. 2. Let the repeat spacing of the bilayer stacking be c . It is well known that for close-packed layers of spheres, there are two ways of arranging the stacking to create periodic arrays of minimum interstitial volume, i.e., the ABCABC... stacking (see Fig. 2 A, bottom) corresponding to the cubic close-packed structure, or, alternatively, the ABAB... stacking corresponding to the hexagonal close-packed structure (Kittel, 1971). In our case, there is no obvious reason for the bilayers to stack in the manner of close-packed spheres. Yet the diffraction pattern shown in Fig. 2 A is exactly that of ABC stacking. The crystal axes of ABC stacking (Fig. 2 A, bottom) are

$$a_1 = (a, 0, 0), a_2 = \left(-\frac{a}{2}, \frac{\sqrt{3}}{2}a, 0 \right), a_3 = \left(\frac{a}{2}, \frac{a}{2\sqrt{3}}, c \right). \quad (1)$$

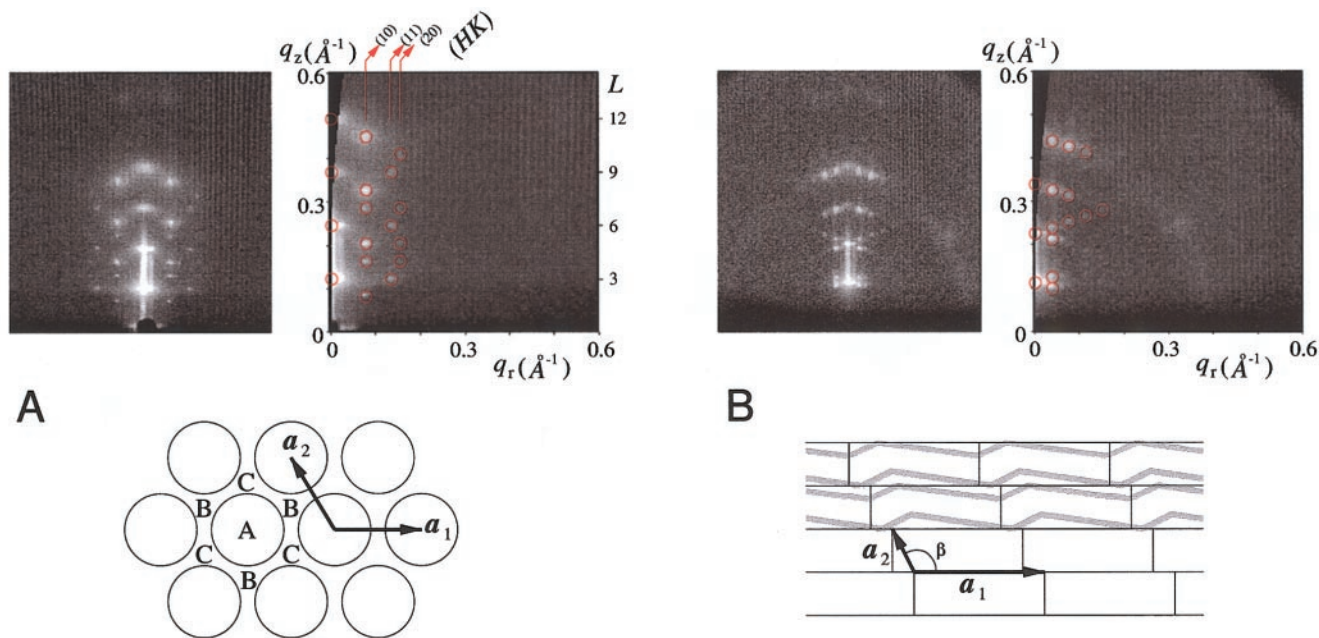


FIGURE 2 X-ray diffraction patterns of magainin in 3:1 DMPC/DMPG ($P/L = 1/30$). The patterns are the same as those produced by magainin in pure DMPC bilayers but stronger in intensity. (A) The crystalline phase of hexagonal ABC stacking is shown on the detector (left) and translated to the q_z - q_r plane (right). The bottom shows a hexagonal close-packed layer of pores (circles), with centers marked A. A second and identical layer can be placed over the first, with centers over the points marked B. There are two nonequivalent choices for a third layer; it can go in over A or over C. The data are consistent with the ABCABC... packing. The reciprocal lattice points generated by ABC packing are shown in red circles on the q_z - q_r plane; they coincide precisely with the data points. The hexagonal indices $HK \cdot L$ for the reciprocal lattice points are also labeled. (B) The crystalline phase of 2D monoclinic is shown on the detector (left) and translated on the q_z - q_r plane (right). The bottom shows the unit cells of 2D monoclinic lattice, that has the same symmetry as the modulated lamellar (rippled) phase P_β , shown schematically in gray lines (Wack and Webb, 1989). The reciprocal lattice points generated by 2D monoclinic lattice are shown in red circles on the q_z - q_r plane; they coincide precisely with the data points.

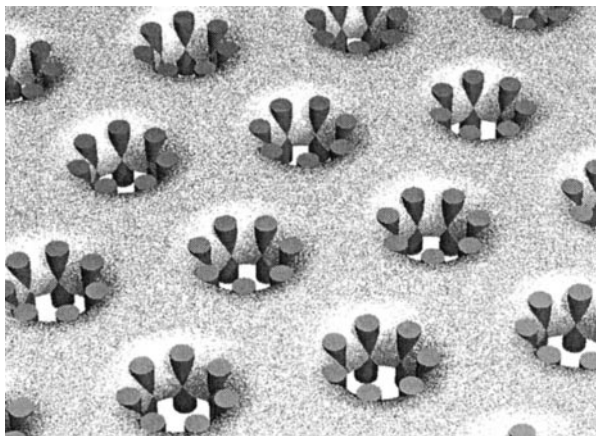


FIGURE 3 A schematic of magainin pores in a lipid bilayer crystallized into a regular hexagonal lattice. The size of the pores and the lattice constant are according to the data. The pore structure was a conjecture based on indirect evidence (Ludtke et al., 1996) in which the toroidal pores of lipid bilayer are stabilized by the magainin monomers (the cylinders) packed in the lipid head group region. Note that we assume that the pores are rotationally disordered.

Hence, the corresponding reciprocal vectors (Warren, 1969) are

$$b_1 = \left(\frac{1}{a}, \frac{1}{\sqrt{3}a}, \frac{-2}{3c} \right), \quad b_2 = \left(0, \frac{2}{\sqrt{3}a}, \frac{-1}{3c} \right), \quad (2)$$

$$b_3 = \left(0, 0, \frac{1}{c} \right).$$

The reciprocal lattice points generated by Eq. 2 are shown in Fig. 2 A, right. They coincide precisely with the diffraction peaks. Note that for close-packed spheres, c is related to a by $c = \sqrt{2/3}a$. In our case there is no apparent relation between c and a , and the space lattice is not cubic. We will call it the hexagonal ABC stacking.

2D monoclinic

The pattern shown in the right panel of Fig. 1 B_1 was reexamined by x-ray over a wider q range. The resulted diffraction pattern on the area detector is shown in Fig. 2 B, left, and translated to the q_z - q_r plane in Fig. 2 B, right. The pattern conforms to the symmetry of a 2D monoclinic lattice, described by the crystal axes:

$$a_1 = (a, 0, 0), \quad a_3 = (c \cot \beta, 0, c), \quad (3)$$

where β is the monoclinic angle. The corresponding reciprocal vectors (Warren, 1969) are

$$b_1 = \left(\frac{1}{a}, 0, \frac{-\cot \beta}{a} \right), \quad b_3 = \left(0, 0, \frac{1}{c} \right). \quad (4)$$

All the diffraction peaks coincide with the reciprocal lattice points generated by the vectors of Eq. 4 (Fig. 2 B). This pattern is the same as the modulated lamellar (rippled) phase $P_{\beta'}$ of phospholipids (Wack and Webb, 1989). In the rippled phase, c is the period of layer stacking and a is ripple wavelength.

Phase diagrams

Fig. 4 shows preliminary RH-T phase diagrams for magainin and protegrin. The phase boundaries are not well defined due to hysteresis and occasional coexistence of two phases. Note that, for magainin, the sequence of phase appearance when the sample was dehydrated and/or cooled is fluid \rightarrow hexagonal ABC \rightarrow 2D monoclinic. However, for protegrin, the sequence is fluid \rightarrow 2D monoclinic \rightarrow hexagonal ABC. Even more surprising, the phase sequence of the protegrin analogue IB367 is unlike PG-1, but is similar to magainin (not shown). The significance of this phase reversal is unknown at the moment.

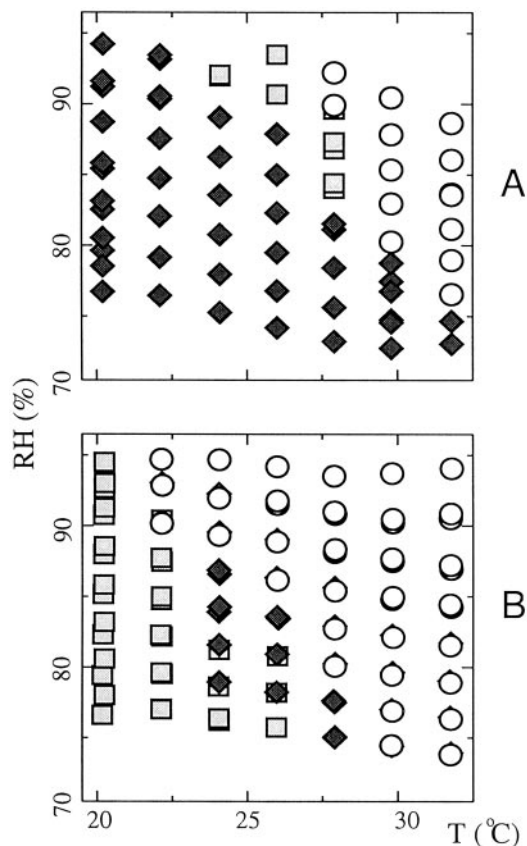


FIGURE 4 RH-T phase diagrams of (A) magainin in DMPC (P/L = 1/30) and (B) protegrin-1 in DMPC (P/L = 1/30). The circles represent the fluid phase in which water-filled pores move randomly in each bilayer (this phase was described in details in Yang, L. et al., 1999). The squares represent the crystalline phase of hexagonal ABC stacking. The diamonds represent the crystalline phase of 2D monoclinic. Overlaid symbols indicate hysteresis.

The phase diagrams show that each crystalline phase covers a substantial range of RH. This will allow us to use the swelling method (Blaurock, 1971) to determine the phases of x-ray diffraction amplitudes. If the pores are rotationally disordered, the unit cell is centrosymmetrical, that is, symmetrical with respect to the inversion transformation. In this case the phase of each diffraction amplitude is either 0 or π , or, equivalently, the amplitude is either positive or negative (Liu et al., 1991). Changing hydration in each phase will vary the period of stacking c and, therefore, vary the q_z of the diffraction peaks. The sign of the amplitude can often be determined by the trend with which the magnitude of the amplitudes varies (Torbet and Wilkins, 1976).

DISCUSSION

The immediate application of these crystalline phases is to obtain the projection structures of the membrane pores. The ultimate structure resolution (or the highest orders of diffraction) obtainable is still unknown. The complete diffraction data, once obtained, can be used to construct the electron density map of the unit cell. The models of the pore can then be compared with the data at the resolution obtained.

It is important to note that neutron, with the use of D_2O , is the only technique capable of detecting the peptide pores in fluid membranes. X-ray diffraction of peptide structures in fluid membranes is very weak, insufficient for analysis. However, the crystalline phases are more easily studied with x-ray because of their shorter wavelength and higher intensity compared with neutron. In principle, the crystalline phases can also be studied with electron microscopy; however, special sample preparations may be required (Reimer, 1997).

The presence of a substrate as a part of an oriented membrane sample presents a problem for x-ray diffraction. As shown in Fig. 2, if the diffraction is measured in the reflection mode, the peaks close to the q_x axis (i.e., $q_z \sim 0$) are not detectable. In contrast, in-plane diffraction is easily obtained by neutrons because the substrate (quartz) is transparent to neutrons, both the reflected and transmitted neutrons are detectable. Unfortunately, crystallographic diffraction with neutrons is impractical due to other problems, such as incoherent scattering and the weakness of neutron beam intensity. In order to obtain the complete x-ray diffraction pattern, we are currently investigating techniques of measurement using the transmission mode.

We thank Michael Zasloff and W. Lee Maloy of Magainin Pharmaceuticals, Inc. and John Fiddes of IntraBiotics Pharmaceuticals, Inc. for their gifts of peptides. H. W. H. was supported by National Institutes of Health grant GM55203 and by the Robert A. Welch Foundation. R. I. L. was supported by National Institutes of Health grants AI37945 and AI22839. We acknowledge the support of the National Institute of Standards and Technology, U.S. Department of Commerce, in providing the neutron

research facilities used in this work, which was also supported by the National Science Foundation under agreement no. DMR-942310.

REFERENCES

- Aumelas, A., M. Mangoni, C. Roumestand, L. Chiche, E. Despau, G. Grassy, B. Calas, and A. Chavanieu. 1996. Synthesis and solution structure of the antimicrobial peptide protegrin-1. *Eur. J. Biochem.* 237:575–583.
- Bessalle, R., A. Kapitkovsky, A. Gorea, I. Shalit, and M. Fridkin. 1990. All-D magainin: chirality, antimicrobial activity and proteolytic resistance. *FEBS Lett.* 274:151–155.
- Blaurock, A. E. 1971. Structure of the nerve myelin membrane: proof of the low resolution profile. *J. Mol. Biol.* 56:35–52.
- Boman, H. G., J. Marsh, and J. A. Goode, eds. 1994. Antimicrobial Peptides. Ciba Foundation Symposium 186. John Wiley and Sons, Chichester, UK. 1–272.
- Chen, F. Y., W. C. Hung, and H. W. Huang. 1997. Critical swelling of phospholipid bilayers. *Phys. Rev. Lett.* 79:4026–4029.
- Cho, Y., J. S. Turner, N. Dinh, and R. I. Lehrer. 1998. Activity of protegrins against yeast-phase *Candida albicans*. *Infect. Immun.* 66:2486–2493.
- Christensen, B., J. Fink, R. B. Merrifield, and D. Mauzerall. 1988. Channel-forming properties of cecropins and related model compounds incorporated into planar lipid membranes. *Proc. Natl. Acad. Sci. USA.* 85:5072–5076.
- Cruciani, R. A., J. L. Barker, M. Zasloff, H.-C. Chen, and O. Colamonic. 1991. Antibiotic magainins exert cytolytic activity against transformed cell lines through channel formation. *Proc. Natl. Acad. Sci. USA.* 88:3792–3796.
- Duchohier, H., G. Molle, and G. Spach. 1989. Antimicrobial peptide magainin 1 from *Xenopus* skin forms anion-permeable channels in planar lipid bilayers. *Biophys. J.* 56:1017–1021.
- Fahrner, R. L., T. Dieckmann, S. S. L. Harwig, R. I. Lehrer, D. Eisenberg, and J. Feigon. 1996. Solution structure of protegrin-1, a broad-spectrum antimicrobial peptide from porcine leukocytes. *Chem. Biol.* 3:543–550.
- Ganz, T., and R. I. Lehrer. 1998. Antimicrobial peptides of vertebrates. *Cudrr. Opin. Immun.* 10:41–44.
- Harroun, T. A. 1999. Hydrophobic matching and membrane mediated interactions in lipid bilayers. Ph.D. thesis, Rice University, Houston, TX. 1–78.
- Harroun, T. A., W. T. Heller, T. M. Weiss, L. Yang, and H. W. Huang. 1999. Experimental evidence of hydrophobic matching and membrane-mediated interactions in lipid bilayers containing gramicidin. *Biophys. J.* 76:937–945; 1999
- Harwig, S. S. L., Waring, A., Yang, H. J., Cho, Y., Tan, L., and Lehrer, R. I. 1996. Intramolecular disulfide bonds enhance the antimicrobial and lytic activities of protegrins at physiological sodium chloride concentrations. *Eur. J. Biochem.* 240:352–357.
- He, K., S. J. Ludtke, D. L. Worcester, and H. W. Huang. 1995. Antimicrobial peptide pores in membranes detected by neutron in-plane scattering. *Biochemistry.* 34:16764–16769.
- He, K., S. J. Ludtke, D. L. Worcester, and H. W. Huang. 1996a. Neutron scattering in the plane of membranes: structure of alamethicin pores. *Biophys. J.* 70:2659–2666.
- He, K., S. J. Ludtke, W. T. Heller, and H. W. Huang. 1996b. Mechanism of alamethicin insertion into lipid bilayers. *Biophys. J.* 71:2669–2679.
- Heller, W. T., K. He, S. J. Ludtke, T. A. Harroun, and H. W. Huang. 1997. Effect of changing the size of lipid headgroup on peptide insertion into membranes. *Biophys. J.* 73:239–244.
- Heller, W. T., A. J. Waring, R. I. Lehrer, and H. W. Huang. 1998. Multiple states of b-sheet peptide protegrin in lipid bilayers. *Biochemistry.* 37:17331–17338.
- Heller, W. T., A. J. Waring, R. I. Lehrer, T. A. Harroun, T. M. Weiss, L. Yang, and H. W. Huang. 2000. Membrane thinning effect by the b-sheet antimicrobial protegrin. *Biochemistry.* 39:139–145.

- Hoffmann, J. A., F. C. Kafatos, C. A. Janeway, and R. A. B. Ezekowitz. 1999. Phylogenetic perspectives in innate immunity. *Science*. 248: 1313–1318.
- Huang, H. W. 2000. Action of antimicrobial peptides: two-state model. *Biochemistry*. 39:8347–8352.
- Huang, H. W., and G. A. Olah. 1987. Uniformly oriented gramicidin channels embedded in thick monodomain lecithin multilayers. *Biophys. J.* 51:989–992.
- Huang, H. W., and Y. Wu. 1991. Lipid-alamethicin interactions influence alamethicin orientation. *Biophys. J.* 60:1079–1087.
- Kokryakov, V. N., S. S. Harwig, E. A., Panyutich, A. A., Shevchenko, G. M. Aleshina, O. V. Shamova, H. A. Korneva, and R. I. Lehrer. 1993. Protegrins: leukocyte antimicrobial peptides that combine features of corticostatic defensins and tachyplesins. *FEBS Lett.* 327:231–236.
- Kittel, C. 1971. Introduction to Solid State Physics, 4th ed. John Wiley, New York. 28–29.
- Liu, W., T. Y. Teng, Y. Wu, and H. W. Huang. 1991. Phase determination for membrane diffraction by anomalous dispersion. *Acta Cryst. A.* 47: 553–559.
- Ludtke, S. J., K. He, Y. Wu, and H. W. Huang. 1994. Cooperative membrane insertion of magainin correlated with its cytolytic activity. *Biochim. Biophys. Acta.* 1190:181–184.
- Ludtke, S., K. He, and H. W. Huang. 1995. Membrane thinning caused by magainin 2. *Biochemistry*. 34:16764–16769.
- Ludtke, S. J., K. He, W. T. Heller, T. A. Harroun, L. Yang, and H. W. Huang. 1996. Membrane pores induced by magainin. *Biochemistry*. 35:13723–13728.
- Matzuzaki, K., M. Harada, T. Handa, S. Fumakoshi, N. Fujii, H. Yajima, and K. Miyajima. 1989. Magainin 1 induced leakage of entrapped calcein out of negatively-charged lipid vesicles. *Biochim. Biophys. Acta.* 981:130–134.
- Powers, L., and P. S. Pershan. 1977. Monodomain samples of dipalmitoylphosphatidylcholine with varying concentrations of water and other ingredients. *Biophys. J.* 20:137–152.
- Qu, X.-D., S. S. L. Harwig, A. Oren, W. M. Shafer, and R. I. Lehrer. 1996. Susceptibility of *Neisseria gonorrhoeae* to protegrins. *Infect. Immun.* 64:1240–1245.
- Qu, X.-D., S. S. L. Harwig, W. M. Shafer, and R. I. Lehrer. 1997. Protegrin structure and activity against *Neisseria gonorrhoeae*. *Infect. Immun.* 65:636–639.
- Reimer, L. 1997. Transmission Electron Microscopy. Springer, Berlin. 1–16 and 100–104.
- Sokolov, Y., T. Mirzabekov, D. W. Martin, R. I. Lehrer, and B. L. Kagan. 1999. Membrane channel formation by antimicrobial protegrins. *Biochim. Biophys. Acta.* 1420:23–29.
- Steiner, H., D. Hultmark, A. Engstrom, H. Bennish, and H. G. Boman. 1981. Sequence and specificity of two antibacterial proteins involved in insect immunity. *Nature*. 292:246–248.
- Tamamura, H., T. Murakami, S. Horiuchi, K. Sugihara, A. Otaka, W. Takada, T. Ibuka, M. Waki, N. Yamamoto, and N. Fujii. 1995. Synthesis of protegrin-related peptides and their antibacterial and anti-human immunodeficiency virus activity. *Chem. Pharm. Bull.* 43:853–858.
- Torbet, J., and M. H. F. Wilkins. 1976. X-ray diffraction studies of lecithin bilayers. *J. Theor. Biol.* 62:447–458.
- Wack, D. C., and W. W. Webb. 1989. Synchrotron x-ray study of the modulated lamellar phase Pb' in the lecithin-water system. *Phys. Rev. A.* 40:2712–2730.
- Wade, D., A. Boman, B. Wählin, C. M. Drain, D. Andreu, H. G. Boman, and R. B. Merrifield. 1990. All-D amino acid-containing channel-forming antibiotic peptides. *Proc. Natl. Acad. Sci. USA.* 87:4761–4765.
- Warren, B. E. 1969. X-ray Diffraction. Dover, New York. 15–26.
- Williams, R. W., R. Starman, K. M. P. Taylor, K. Cable, T. Beeler, M. Zasloff, and D. Covell. 1990. Raman spectroscopy of synthetic antimicrobial frog peptides magainin 2a and PGLa. *Biochemistry*. 29: 4490–4496.
- Wu, Y., H. W. Huang, and G. A. Olah. 1990. Method of oriented circular dichroism. *Biophys. J.* 57:797–806.
- Wu, Y., K. He, S. J. Ludtke, and H. W. Huang. 1995. X-ray diffraction study of lipid bilayer membrane interacting with amphiphilic helical peptides: diphtanoyl phosphatidylcholine with alamethicin at low concentrations. *Biophys. J.* 68:2361–2369.
- Yang, D., O. Chertov, S. N. Bykovskaia, Q. Chen, M. J. Buffo, J. Shogan, M. Anderson, J. M. Schroder, J. M. Wang, O. M. Z. Howard, and J. J. Oppenheim. 1999. b-Defensins: linking innate and adaptive immunity through dendritic and T cell CCR6. *Science*. 286:525–528.
- Yang, L., T. A. Harroun, W. T. Heller, T. M. Weiss, and H. W. Huang. 1998. Neutron off-plane scattering of aligned membranes. I. Method of measurement. *Biophys. J.* 75:641–645.
- Yang, L., T. M. Weiss, T. A. Harroun, W. T. Heller, and H. W. Huang. 1999. Supramolecular structures of peptide assemblies in membranes by neutron off-plane scattering: method of analysis. *Biophys. J.* 77: 2648–2656.
- Yasin, B., R. I. Lehrer, S. S. L. Harwig, and E. A. Wagar. 1996. Protegrins: structural requirements for inactivating elementary bodies of *Chlamydia trachomatis*. *Infect. Immun.* 64:4863–4866.
- Zasloff, M. 1987. Magainins, a class of antimicrobial peptides from *Xenopus* skin: isolation, characterization of two active forms and partial cDNA sequence of a precursor. *Proc. Natl. Acad. Sci. USA.* 84: 5449–5453.